

Hydrogen Control of Large Bottom-Poured Forging Ingots at Ellwood Quality Steels



Authors

Bjorn Gabrielson (top row, left) retired, Ellwood Group Inc., New Castle, Pa., USA
bjorn.e.gabrielson@gmail.com

Brendan Connolly (top row, right) director of steelmaking technology, Ellwood Quality Steels, New Castle, Pa., USA
bconnolly@elwd.com

Steve Lubinski (middle row, left) manager of laboratory services, Ellwood Quality Steels, New Castle, Pa., USA
slubinski@elwd.com

Sean Cowden (middle row, right) operations engineer, Ellwood National Steel, Irvine, Pa., USA
scowden@elwd.com

Hongliang Yang (bottom) R&D team leader, ABB AB/Metallurgy, Vasteras, Vastmanland, Sweden
hongliang.yang@se.abb.com

Hydrogen removal and hydrogen pickup during liquid steel processing at Ellwood Quality Steels are studied in detail with particular emphasis on the effect of electromagnetic stirring on hydrogen removal. The results of this work indicate that the ultralow-hydrogen practice implemented at Ellwood Quality Steels allows for consistent production of high-quality, large cross-section, bottom-poured steel ingots with hydrogen content of less than 1.5 ppm.

The Ellwood Group operates two separate electric arc furnace (EAF) meltshops, each with a maximum heat size of 47 metric tons:

- Ellwood Quality Steels (EQS) in New Castle, Pa., USA, with a capacity of 390,000 metric tons of plain carbon steel, low- and medium-alloy steel, tool steels and martensitic stainless. Maximum ingot weight at EQS is 170 metric tons.
- Ellwood National Steels (ENS) in Irvine, Pa., USA, with a capacity of 80,000 metric tons of high-alloyed, low-carbon stainless, Ni-based and other sophisticated alloys.¹ Maximum ingot weight at ENS is 90 metric tons.

The EQS meltshop was commissioned in late 1985 with a maximum heat size of 40 metric tons.² The heat size increased gradually to 47 metric tons with the following modifications:

- Original 1985 runner tap EAF replaced with enlarged eccentric bottom tapping (EBT).
- Lengthening of the original ASEA-SKF ladles.
- Optimization of ladle refractory thickness.

With these heat size improvements, the maximum as-cast

bottom-poured forging ingot weight increased to 47 metric tons from a single heat. Production flow at the EQS meltshop is shown in Fig. 1.

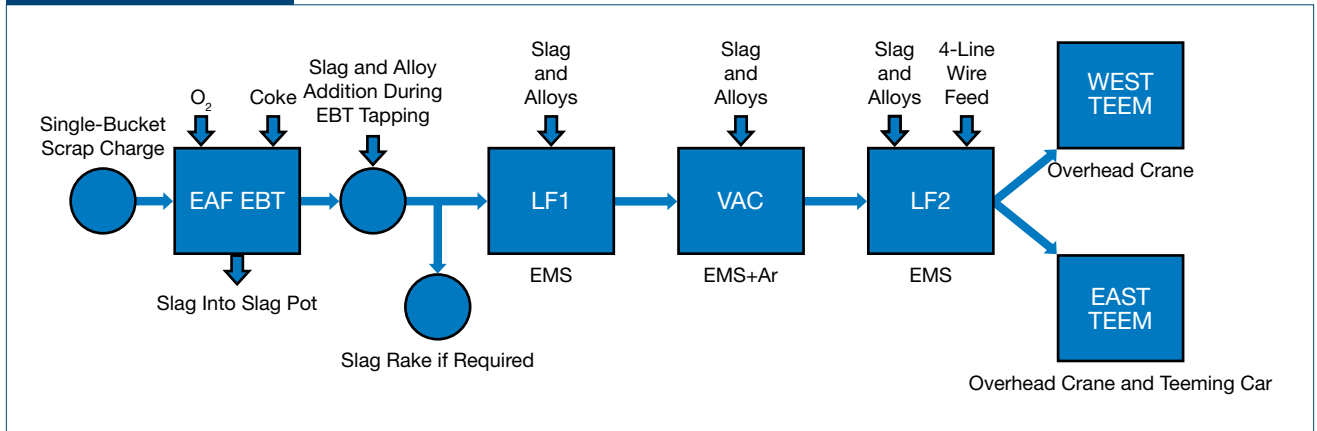
The EQS meltshop has produced roughly 8,300,000 metric tons of forging and ring rolling ingots since start-up in December 1985. There are two teeming bays at EQS:

- West teeming bay for 24- to 47-metric-ton ingots teemed by overhead crane.
- East teeming bay for 2- to 24- and 60- to 170-metric-ton ingots.

The EAF, ladle furnace No. 1 (LF1), vacuum station, ladle furnace No. 2 (LF2) and chemical laboratory (located between EAF and LF1) are very compact with a total steelmaking platform length of only 85 m. Both ladle furnaces are equipped with electromagnetic stirring (EMS) in order to allow for short-arc reheating under a fully liquid reducing slag cover. This makes it possible for EQS to consistently produce extremely clean steel with very tight composition control while maintaining high productivity.³ Table 1 lists some key performance indicators (KPIs) for 2017.

The sandwich pouring process was implemented at EQS in 2015 in order to produce up to 170-metric-ton ingots using four ladles of liquid steel. Sandwich pouring is shown

Figure 1



Production flow at Ellwood Quality Steels (EQS) meltshop.

schematically in Fig. 2. The development work and excellent quality results of sandwich-poured, large cross-section ingots at EQS are well documented.⁴

Hydrogen in Steel

It was recognized in the early 20th century that certain internal hairline cracks in large steel forgings were related to hydrogen.⁵ These cracks have been termed “hydrogen flakes” and extensive research on their formation and prevention has been performed by both academia and industry.

Hydrogen is present in steel as a monatomic species with high diffusivity and low solubility in low-temperature-transformation products. The mechanism for hydrogen flake formation remains controversial, however calculations have been performed⁶ to show that the pressure buildup due to hydrogen within a steel matrix is easily high enough to exceed that which even a high-strength steel is able to withstand.

The atomic fraction of hydrogen in equilibrium with H₂ gas at pressure P (atm) is given as:⁷

$$C_0 = 0.00185 \sqrt{Pe}^{\frac{-3440}{T}} \quad (\text{Eq. 1})$$

where C_0 is the atom fraction of hydrogen and T is in Kelvin. P must be replaced by fugacity at the pressures being considered. An approximation of the Taylor expansion can be used to estimate fugacity, f :

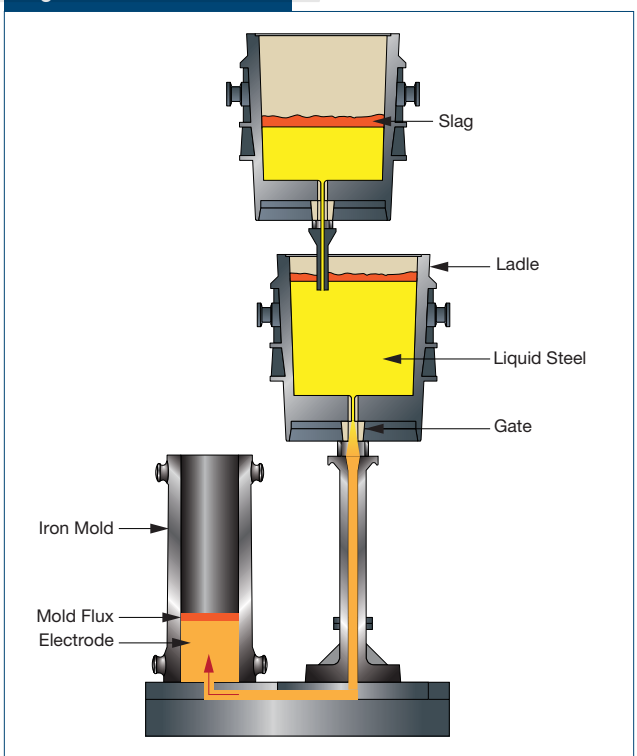
$$f \approx \frac{P^2 \bar{V}}{RT} \quad (\text{Eq. 2})$$

Table 1

Key Performance Indicators, 2017

KPI	Value
EAF gross tap-to-tap time	52.7 minutes/heat
EAF power-on time	36.1 minutes/heat
EAF power-off time	16.6 minutes/heat
Productivity	27.3 heat/day

Figure 2



Schematic of sandwich pouring process.

where \bar{V} is the molar volume and R is the gas constant. In order to determine the molar volume, the van der Waals equation of state for one mole of gas can be used:

$$\left(P + \frac{a}{V^2}\right)(V - b) = RT \quad (\text{Eq. 3})$$

$$a = \frac{27R^2T_{crit}^2}{64P_{crit}} \quad (\text{Eq. 4})$$

$$b = \frac{RT_{crit}}{8P_{crit}} \quad (\text{Eq. 5})$$

After determining the fugacity, the pressure and molar volume can be simultaneously solved. Fig. 3 shows the internal pressure buildup versus various amounts of hydrogen in the steel matrix at different temperatures. Fig. 4 shows the difference in relative volumes of steel, hydrogen gas, and water at standard temperature and pressure.

The important point from Figs. 3 and 4 is that even at a hydrogen content of 1 ppm, coming from a very small relative volume of water, the matrix will be unable to withstand the high internal pressure buildup at room temperature. The hydrogen present within the steel must be accommodated in some fashion. Hydrogen accumulates at voids and interfaces within the steel, thereby lowering the hydrogen dissolved within the matrix. Grain boundaries, dislocations,

microporosity and inclusions are all potential trapping sites where hydrogen is able to diffuse out of the matrix and remain in these traps without detrimental flakes occurring.⁷ Fully dense forgings with low inclusion content are more susceptible to hydrogen flaking due to the reduced availability of trapping sites.

Hydrogen can be removed from steel forgings by subcritical diffusion annealing in order to prevent hydrogen flaking. However, the diffusion annealing practice is both time-consuming and expensive. Fig. 5 shows the required diffusion annealing time versus the forging diameter for removal of 50% of the original hydrogen content at 650°C according to Thelning's calculation.⁸ The diffusion annealing time required for hydrogen removal in large cross-section forgings is prohibitively long.

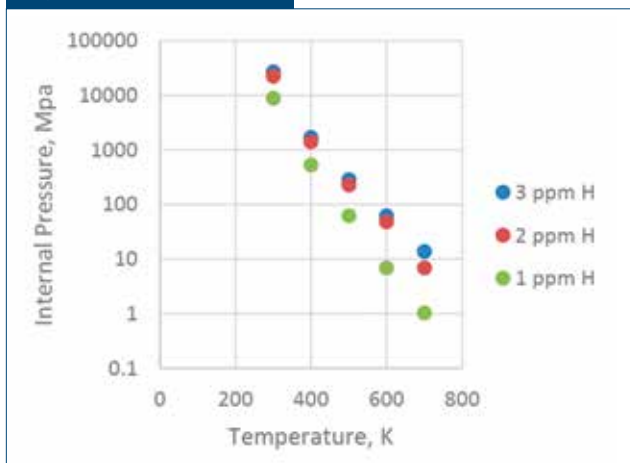
EQS Vacuum Station

The secondary steelmaking operation at EQS utilizes a vacuum hood degassing station with combined argon gas and EMS for fast and efficient hydrogen removal from the liquid steel. The EMS was upgraded from 1,000 A max current to 1,350 A max current in 1998. The EQS vacuum station is shown schematically in Fig. 6.

Typical operating pressure of less than 1 mbar above the liquid steel bath is consistently achieved using a four-stage steam ejector vacuum pump. The four-stage steam ejector vacuum pump utilizes parallel ejectors in the first two pumping stages in order to achieve the highest possible pumping capacity and reach operating pressure in less than four minutes.

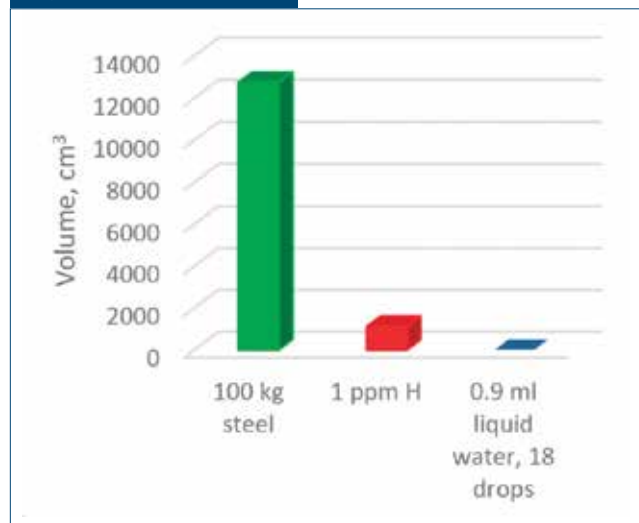
It is common for steam ejector pumps used in the vacuum treatment of liquid steel to require periodic

Figure 3



Internal pressure buildup from hydrogen.

Figure 4



Steel, hydrogen and water volume.

high-pressure water jet cleaning in order to remove the buildup of concrete-like deposits of process dust inside the pump itself. EQS installed an in-line vacuum bag filter in 2004 between the vacuum station and the vacuum pump in order to separate the process dust that is generated by evaporation and condensation of low-vapor-pressure elements such as magnesium, zinc and manganese.⁹ The dust is highly pyrophoric and will combust readily if exposed to oxygen. The bags are cleaned by nitrogen pulse jet after each vacuum treatment and the dust is collected in a nitrogen pneumatic ejection dispenser at the bottom of the bag filter. At the end of the bag cleaning cycle, the dust is ejected into the ladle furnace offgas system where it is combusted and then captured by the ladle furnace baghouse. The in-line vacuum bag filter has provided several advantages for the EQS secondary steelmaking operation:

- No degradation of vacuum capacity or vacuum pressure due to dust buildup in the pump over time.
- No cleaning (downtime) of the vacuum pump is required.
- No manual handling of the pyrophoric dust is required.

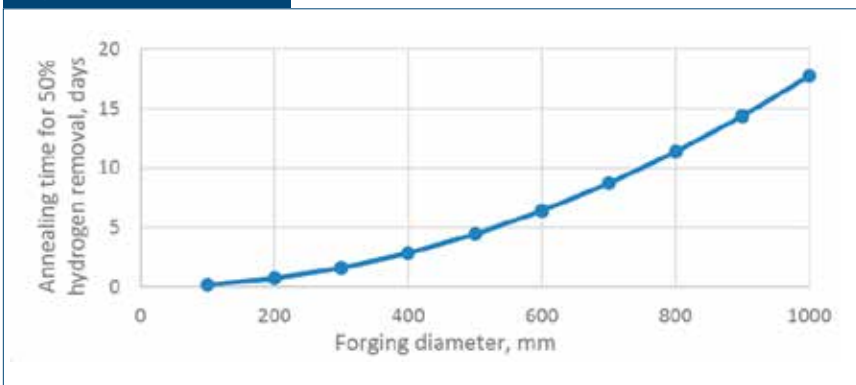
Hydrogen Sampling

EQS performs hydrogen sampling a minimum of two times for every heat produced. The first sample is taken from the ladle after vacuum treatment to ensure the process achieved the necessary low hydrogen content prior to bottom pouring. The final sample, which is used for certification, is taken from the ingot mold when the mold is almost full to ensure that the hydrogen content reported to customers is accurate and includes any hydrogen pickup that occurs during post-vacuum treatment secondary steelmaking operations and bottom pouring.

Standard hydrogen sampling and analysis at EQS has been previously described and proven to be an accurate method.^{3,10} The standard method at EQS is:

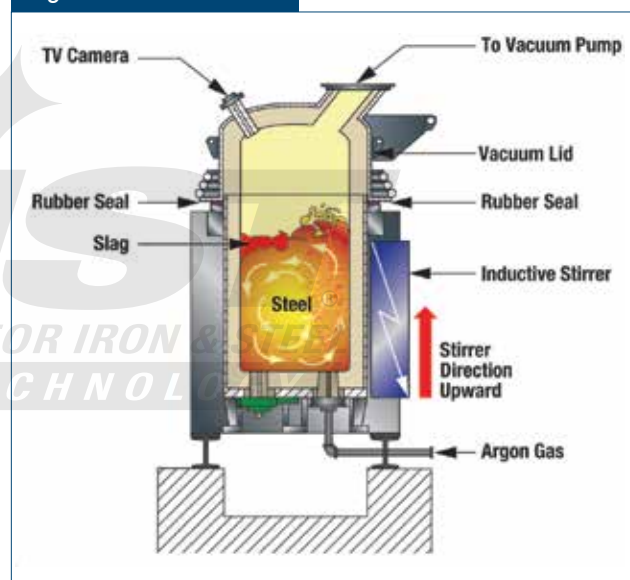
- Liquid metal sampling by evacuated 6-mm diameter glass pin tube.
- Immediate, rapid quenching of the pin with cold, clean water.
- Storage of the pin in dry ice until analysis (analyzed within 24 hours).

Figure 5



Diffusion time for 50% hydrogen removal.

Figure 6



Schematic of vacuum hood degassing station at EQS.

- 3–5 g samples broken from the pin while cold.
- Hot extraction analysis at 1,100°C using a LECO hydrogen analyzer.

Hydrogen Removal

The amount of hydrogen dissolved in liquid steel is proportional to the square root of the partial pressure of hydrogen in contact with the liquid steel according to Sievert's Law. Removal of hydrogen from the liquid steel is achieved by exposing the liquid steel to an atmosphere of reduced hydrogen partial pressure. The amount of hydrogen removed from the liquid steel depends on the following factors:¹⁰

Table 2

Computational Fluid Dynamics (CFD) Modeling Parameters

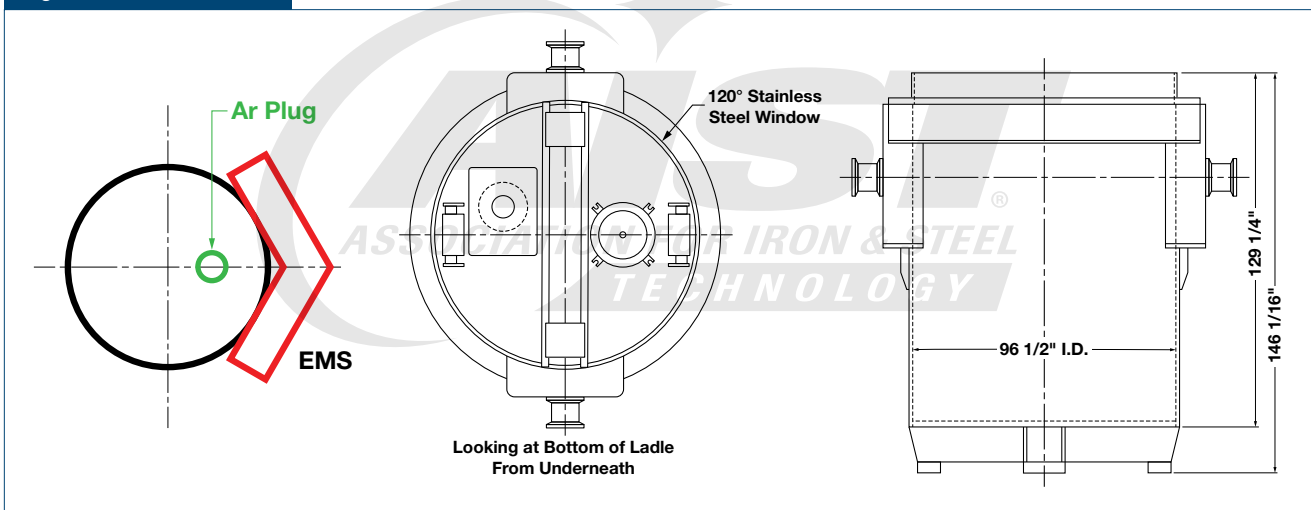
Parameter	Case 1	Case 2	Case 3
Heat size, metric tons	45	45	45
EMS type	None	ORT34	ORT34
EMS Current, A	0	1,000	1,350
EMS stir direction	Up	Up	Up
Vacuum pressure, mbar	1	1	1
Ar flowrate, NI/min	80	80	80
Slag amount, kg	600	600	600

- Mass transfer coefficient of hydrogen, kH , which depends on flow conditions in the liquid steel.
- Ratio between the free metal surface area and the volume of liquid steel.

- Vacuum treatment time.
- Hydrogen concentration difference relative to equilibrium with the partial pressure above the liquid steel according to Sievert's Law.
- Stirring gas flowrate and hydrogen concentration difference relative to equilibrium with the partial pressure in the stirring gas according to Sievert's Law.
- Concentration of surface active elements such as sulfur and oxygen in the liquid steel.

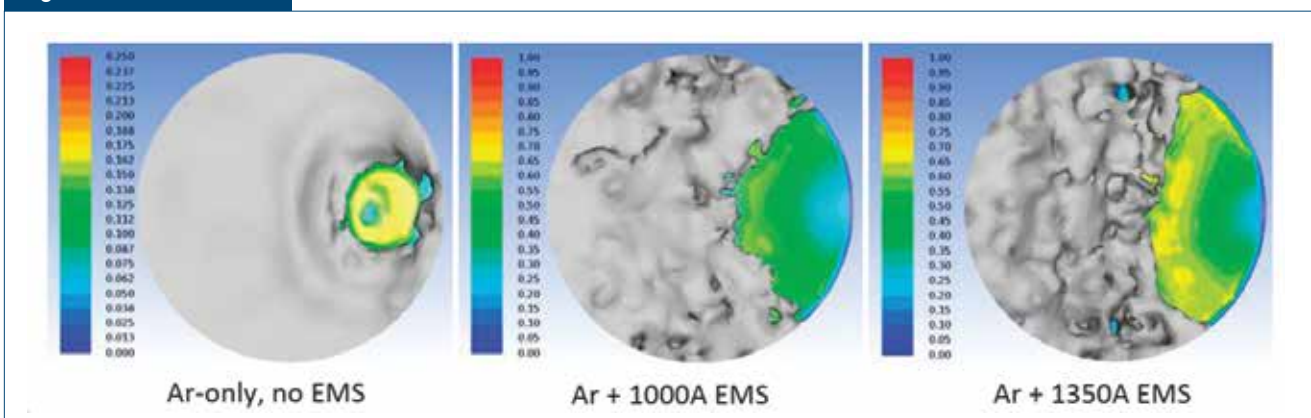
Computational Fluid Dynamics (CFD) Simulations — Stirring power density due to Ar gas and EMS during vacuum treatment affects several of the factors listed above. Simulations were performed by ABB R&D Metallurgy to evaluate how different stirring parameters will influence the important factors for

Figure 7



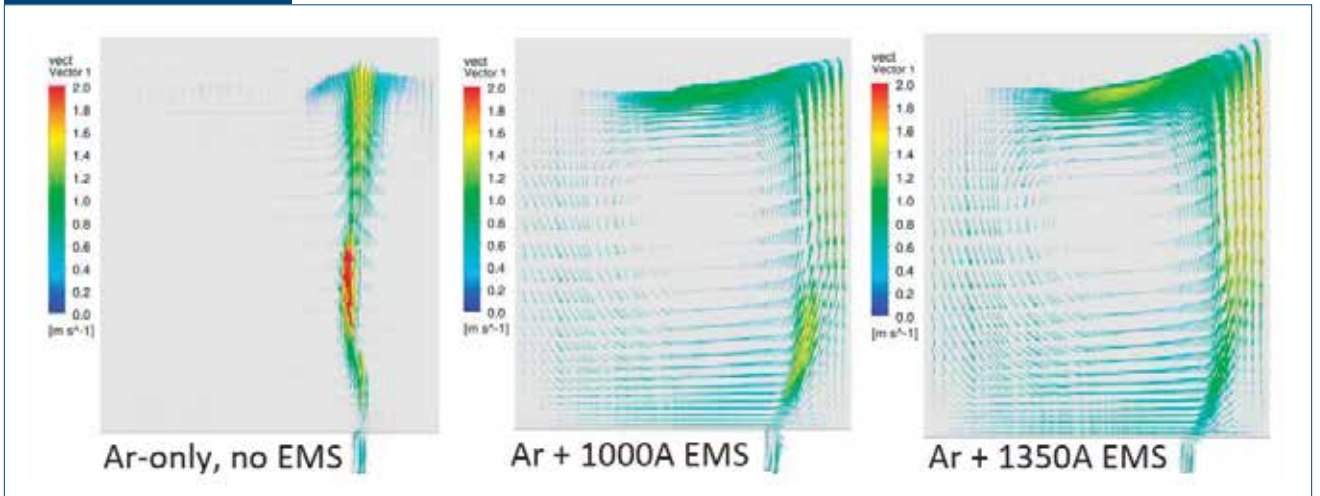
Ladle, argon plug and electromagnetic stirring configuration.

Figure 8



Computational fluid dynamics (CFD) modeling results for top surface liquid metal exposure and velocity (m/s).

Figure 9



CFD modeling results for liquid metal velocity.

hydrogen removal. Three cases were simulated as shown in Table 2.

Fig. 7 shows the argon gas plug location, ladle geometry and location of the ORT34 electromagnetic stirrer. The Ar gas plug is located on the EMS side, $1/2$ radius of the working lining inside diameter.

Fig. 8 shows the results of the CFD simulation for the top surface of the liquid slag and steel for Cases 1–3. Fig. 9 shows the liquid metal velocity vectors through the ladle cross-section for Cases 1–3. The benefits of combined argon gas and EMS with the maximum EMS current (1,350 A) are as follows:

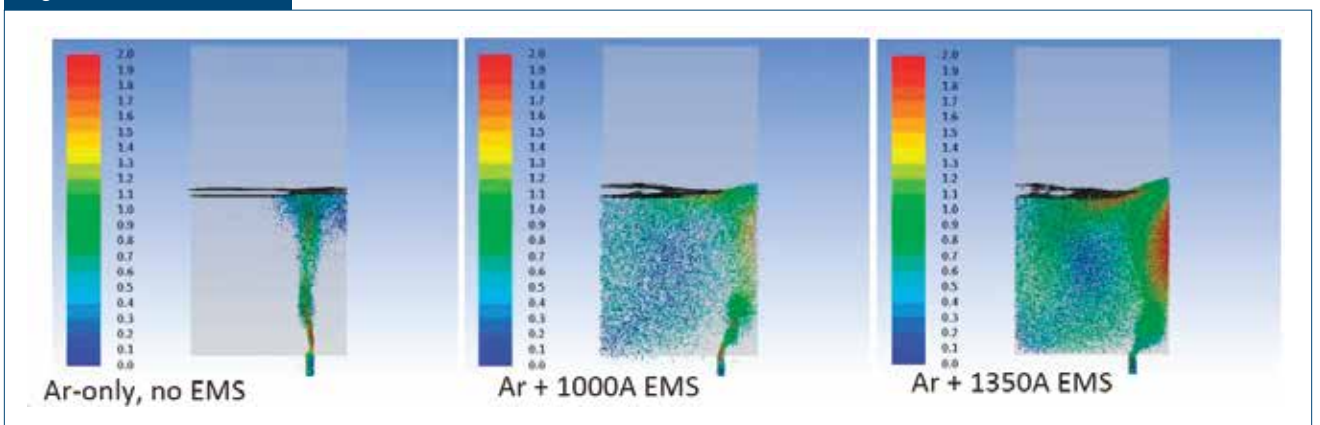
- Free metal surface exposure to the low-pressure atmosphere is increased.
- Liquid metal velocity at the free metal surface is increased.
- Bulk liquid metal flow (mixing) is increased.

The increased liquid metal velocity for Cases 2 and 3 also aids in dispersing argon gas bubbles throughout the liquid metal. Fig. 10 shows the argon bubble distribution within the liquid steel, with the color of each bubble indicating its velocity. Dispersion of the argon bubbles throughout the melt is beneficial for the hydrogen removal process for the following reasons:

- Maximization of the bubble retention time to achieve, as close as possible, equilibrium hydrogen content in each bubble according to Sievert's Law.
- Exposure of bulk liquid to the argon bubbles rather than only in a narrow stream of argon.

The results of ABB's CFD modeling are summarized in Table 3. The combined argon gas and EMS

Figure 10



CFD results for Ar bubble dispersion and velocity (m/s).

Table 3

Summary of CFD Modeling Results From ABB

Result	Case 1 (Ar gas only)	Case 2 (Ar gas + 1,000 A EMS)	Case 3 (Ar gas + 1,350 A EMS)
Stirring power density, W/ton	65	600	700
Free metal surface, %	7.40	22.50	27.90
Average surface velocity, m/s	0.14	0.41	0.53
Average bulk metal velocity, m/s	0.11	0.48	0.71

at 1,350 A provides superior conditions for hydrogen removal during vacuum treatment.

CFD Model Verification — Several verification tests were performed in order to confirm the results of the CFD modeling:

Mixing Time Comparison: A mixing time comparison of combined argon and EMS versus argon-only stirring was performed by Gabrielson and Lubinski in 1988¹⁰ using a 1,000-amp electromagnetic stirrer. The comparison is extended in this work to include the 1,350-amp electromagnetic stirrer currently installed at EQS. The mixing time study was performed with Cu as a tracer element. 5 kg Cu/t steel was added to the ladle followed by chemical sampling every 10 seconds. Due to the practical limitations of obtaining chemical samples during vacuum treatment, the mixing

time study must be performed at atmospheric pressure. The argon gas flowrate was adjusted to compensate for the loss of mechanical stirring power of the Ar gas expansion at a vacuum pressure of 2 mbar for consistency with the previous work. Sundberg's formula¹¹ for calculating power through isothermal expansion of the gas is:

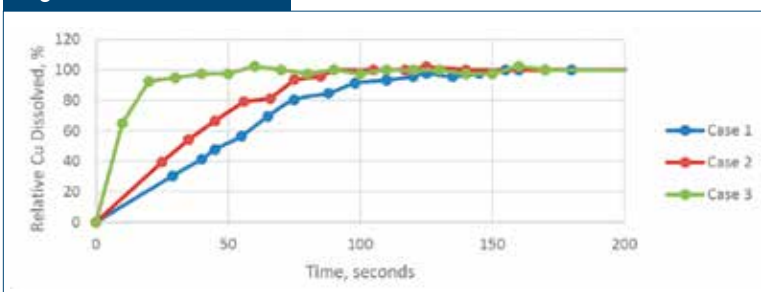
$$P_{mech} = \frac{387QT_1 \left[\left(1 - \frac{T_0}{T_1} \right) + \ln \frac{P_1}{P_2} \right]}{M_L} \quad (\text{Eq. 6})$$

where

P_{mech} = the mechanical stirring power density (W/t),
 Q = the argon gas flowrate (Nm³/second),
 T_1 = the steel temperature (K),
 T_0 = room temperature (K),
 P_1 = the pressure at the ladle bottom (Pa),
 P_2 = the pressure above the liquid surface (Pa) and
 M_L = the liquid metal weight (ton).

Fig. 11 shows the results of the mixing time trials. These experimental results confirm superior liquid steel mixing with combined Ar gas and 1,350 A EMS currently installed at EQS, as predicted by the CFD modeling.

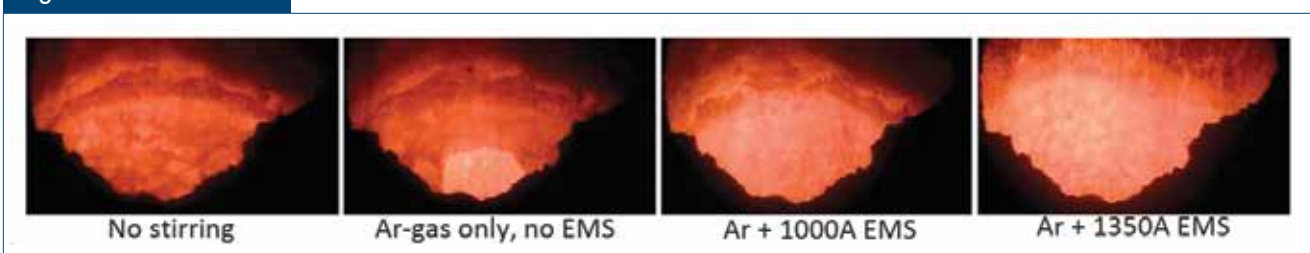
Figure 11



Copper tracer mixing time results.

Free Metal Surface Comparison: The CFD modeling results for free metal surface were tested with trials at the EQS vacuum station using the stirring parameters as indicated in Table 2, with the exception of argon flowrate. Due to the camera view angle at the EQS vacuum station, it is not possible to see the entire liquid surface during vacuum treatment. At typical argon flowrate of 80 NI/minute the visible area shows nearly 100% exposed liquid steel. In order to show the difference in surface area exposure, the argon flowrate

Figure 12



Camera view images for different stirring at EQS vacuum station.

for this trial was reduced to 60 NI/minute. Images from the vacuum station for each case (and also without Ar gas or EMS) are shown in Fig. 12, where the increased free metal surface for combined induction and argon stirring was recorded utilizing a CCTV mounted in the vacuum hood (see Fig. 6).

Hydrogen Removal Comparison: 85 heats were produced without the use of EMS during vacuum treatment. The trial parameters were as follows:

- Vacuum pressure <1.0 mbar.
- Vacuum treatment time minimum 20 minutes.

Table 4 shows the results of this trial compared to heats using EMS that met the same parameter requirements above during 2017. A histogram of the hydrogen values after vacuum treatment is shown in Fig. 13. The average vacuum pressure was slightly lower for the case of combined Ar gas + EMS stirring, however this would only account for about 0.02 ppm difference in equilibrium hydrogen according to Sievert's Law. Combined Ar gas and EMS significantly improves the exposed liquid steel surface, bulk mixing and Ar gas bubble retention time, giving consistently lower post-vacuum hydrogen content.

Hydrogen Removal Results — Vacuum treatment (typically at <1 mbar pressure) is performed on every heat produced at EQS. Vacuum treatment time ranges from 10 to 30 minutes depending on the steel grade and cross-section being produced. The average hydrogen content in the ladle after vacuum treatment with combined Ar gas and EMS stirring at EQS is shown from 2014–2018 in Fig. 14. Continuous improvement efforts by EQS steelmaking and maintenance departments have been effective in maximizing the vacuum station efficiency.

Hydrogen Pickup

After vacuum treatment is complete, the liquid steel must be protected from hydrogen sources such as moisture and hydrocarbons. In the secondary steelmaking operation at EQS, the primary hydrogen sources after vacuum treatment are atmospheric moisture and moisture present in alloying additions. Atmospheric moisture is controlled by maintaining complete coverage of the bath with a liquid slag layer during post-vacuum secondary steelmaking operations. This is possible even

Table 4

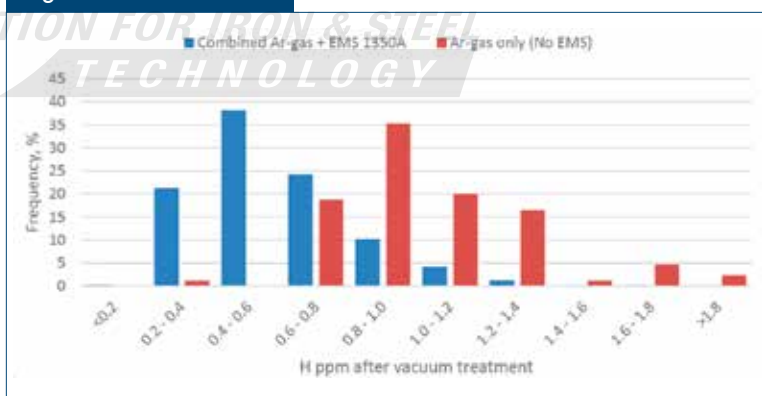
Results of Ar Gas-Only Stirring Trial vs. Combined Ar Gas + EMS 1350A

Parameter	Ar gas only (No EMS)	Combined Ar gas + EMS 1350A
Number of heats	85	3,256
Average pressure, mbar	0.77	0.72
Average time, minutes	27	27
Average H after vacuum treatment, ppm	1.05	0.59

during reheating at the ladle furnace due to EMS without breaking the slag cover. All potential sources of hydrogen such as argon stirring, alloying additions and slag additions are strictly controlled after vacuum treatment.

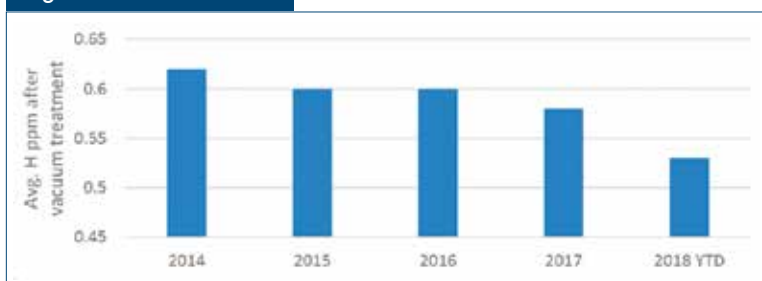
Hydrogen is tested after vacuum treatment for every heat produced at EQS in order to ensure that the necessary hydrogen removal was achieved. An additional hydrogen test was taken from the ladle just prior to bottom pouring on 190 heats and compared to the test taken immediately after vacuum treatment

Figure 13



Post-vacuum treatment hydrogen for Ar gas-only stirring vs. combined Ar gas + EMS.

Figure 14



Average hydrogen after vacuum treatment by year.

Table 5

Typical Replacement Life for Ladle and Slidegate Refractory Components

Component	Component life (heats per replacement)
Ladle brick (barrel + slagline)	80
Inner nozzle	15–20
Slidegate plates	5
Collector nozzle	5

in order to verify that the post-vacuum treatment secondary steelmaking operations do not make a significant contribution to the hydrogen pickup. The results of this trial showed an average of <0.1 ppm higher hydrogen in the test just prior to bottom pouring, which confirms that there is no significant hydrogen pickup during the post-vacuum treatment secondary steelmaking processes at EQS.

During the teeming operation, there are several sources of hydrogen pickup:

- Ladle slidegate refractory components.
- Atmospheric moisture.
- Bottom-pour tile and mortar cover.
- Teeming flux.

The influence of these various hydrogen sources on hydrogen pickup during bottom pouring were investigated in detail using data collected and analyzed for more than 30,000 heats produced at EQS.

Ladle Slidegate Refractory Components — The ladle slidegate refractory components include the ladle inner nozzle, slidegate plates and collector nozzle. Typical life for various ladle and slidegate refractory components is listed in Table 5.

Fig. 15 shows the average relative hydrogen pickup for the first five heats on a new ladle (all components from Table 5 replaced for first heat on ladle) and for heats where only the inner nozzle or slidegate plate/

collector were replaced. Note that the slidegate plates and collector nozzle are always replaced when the inner nozzle is replaced.

Hydrogen pickup for a brand-new ladle compared to a new inner nozzle and slidegate plates is identical, which indicates that the newly relined ladle has no impact beyond the new inner nozzle and slidegate components. This is due to vacuum treatment after initial exposure of the barrel and slagline to the liquid steel. The largest contribution to hydrogen pickup from these refractory components is due to changing the slidegate plates and collector nozzle, accounting for up to 17% of the hydrogen pickup. EQS has specific ladle refractory requirements in place for hydrogen-critical heats as part of the “ultralow-hydrogen practice” in order to ensure minimal hydrogen pickup from new refractory components.

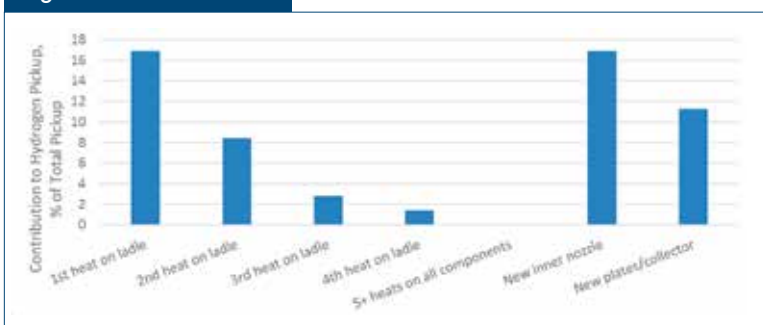
Atmospheric Moisture — Atmospheric moisture can have a significant contribution to hydrogen pickup during bottom pouring if the liquid steel stream is not protected from contact with the atmosphere. Argon shrouding is performed on all heats produced at EQS, with the exception of specific grades where particular customer requirements will not allow this practice.

The benefits of argon shrouding are more pronounced during hot, humid weather due to the additional moisture in the atmosphere. The relative hydrogen pickup for non-shrouded and shrouded heats produced since 2015 are shown by month along with average monthly humidity in Fig. 16. Relative hydrogen pickup is expressed as percentage of average (100% being the average of all heats). Argon shrouding results, on average, gave 35% lower hydrogen pickup compared to non-shrouded heats.

The EQS argon shroud design was improved significantly at the end of 2015. The new argon shroud design allows for 100% sealing of the liquid metal stream from the atmosphere and positive pressure of argon within the shroud. Oxygen testing within the argon shroud during actual teeming operations confirmed oxygen levels below 0.5%, indicating that atmospheric exposure is reduced by more than 97% when the EQS shroud is utilized.

In the production of large ingots (>47 metric tons) where the sandwich pouring process is used to pour more than one ladle of liquid steel into a single mold, the liquid stream from the top ladle(s) is completely protected from the atmosphere by a ladle-to-ladle shroud. The shroud is submerged into the liquid bath of the lower ladle for the entire duration of pouring from the upper ladle.⁴

Figure 15



Effect of slidegate refractory status on hydrogen pickup.

Bottom-Pour Tile and Mortar Cover — Refractory bottom-pour tile contains

some small amount of moisture that is absorbed after production during packaging, transport and storage. Moisture content testing of EQS bottom-pour tile confirmed that the practice of sealed pallet, dry storage prevents any significant moisture pickup in the bottom-pour tile during storage.

One source of moisture to the bottom-pour tile is the refractory mortar that is used for compression of the tiles once they are set in the sprue plate. The refractory mortar is an olivine-based material that is mixed with 5–10% water in the bottom pour plate preparation area and evenly applied on top of the runner brick channel after bricks have been set. When the refractory mortar is cured by the hot sprue plate it turns very hard, locking all of the bottom-pour tiles together and assisting in compression.

A hygrometer was placed inside the bottom-pour tile in order to measure the specific humidity (g H₂O/kg air) within the bottom-pour setup. A separate hygrometer was placed in the open atmosphere for comparison. Fig. 17 shows that the humidity inside bottom-pour tile initially is decreasing when the tiles are first set, likely due to the heating of the tiles by the hot sprue plate driving off residual moisture. When the mortar is applied to the brick there is a significant increase in the specific humidity.

This increase in specific humidity within the bottom-pour system presented a potential source of hydrogen pickup. Ohmori et al.¹² found that pre-heating the bottom-pour tile with dry forced air can reduce the moisture content of the refractory and reduce hydrogen pickup. EQS has developed and implemented a bottom-pour tile pre-heating system that is used for the production of all large (>47 metric tons) ingots. The pre-heating system is capable to reach air temperatures of 500°C in order to drive all moisture out of the refractory bottom-pour system.

Teeming Flux — The teeming flux used during bottom pouring at EQS contains approximately 0.25% moisture by weight according to recent analyses. At EQS, the teeming flux addition is based on the ingot cross-section and total volume. Fig. 18 shows the average grams of hydrogen pickup versus the grams hydrogen present in the teeming flux moisture for various ingot sizes produced at EQS. The data set excludes heats with new slidegate or inner nozzle refractory components. Hydrogen pickup correlates strongly with the hydrogen present in the teeming flux.

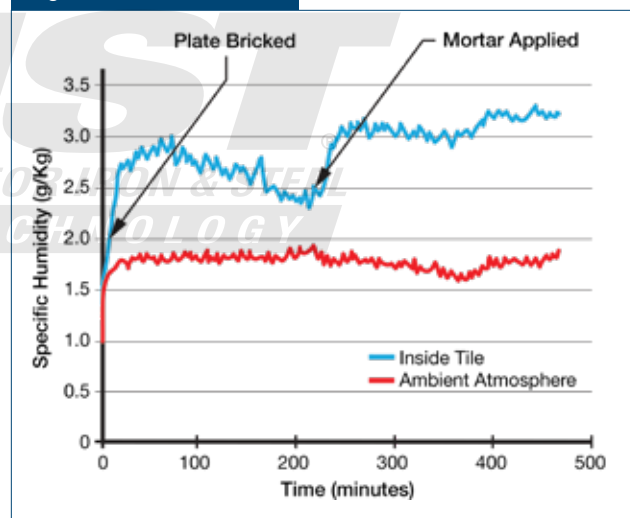
Figure 16



Hydrogen pickup vs. humidity by month.

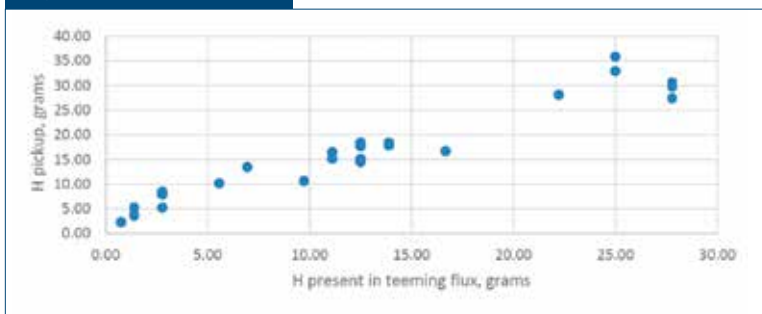
When using molds that have been adequately pre-heated, EQS has found that application of flux by pouring directly into the hot mold allows removal of some residual moisture from the flux and results in ~8% reduction in the hydrogen pickup. This flux

Figure 17



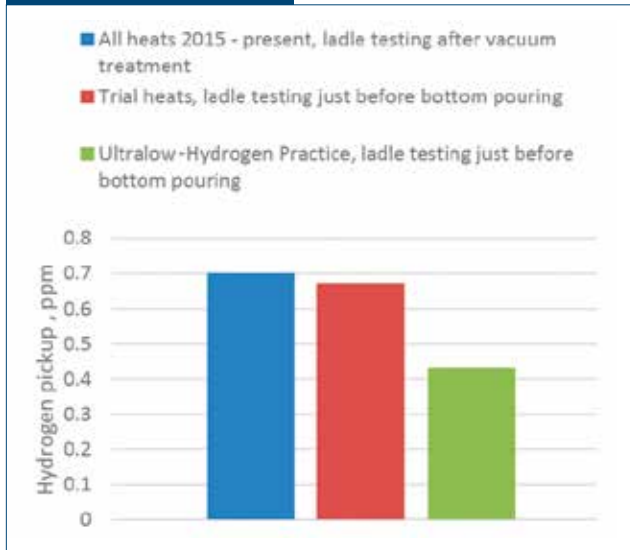
Specific humidity increase from application of compression mortar.

Figure 18



Hydrogen pickup vs. hydrogen present in teeming flux.

Figure 19



Hydrogen pickup for standard and ultralow-hydrogen practice.

application method has been incorporated into the ultralow-hydrogen practice.

Results and Conclusion

The EQS secondary steelmaking processes consistently deliver high-quality, low-hydrogen liquid steel to the teeming bay. Standard practices in the bottom-pouring operation minimize hydrogen pickup during routine operation. In the production of large ingots (>47 metric tons) where sensitivity to hydrogen becomes even more significant, special ultralow-hydrogen practices are in place to ensure <1.5 ppm H in the final ingot:

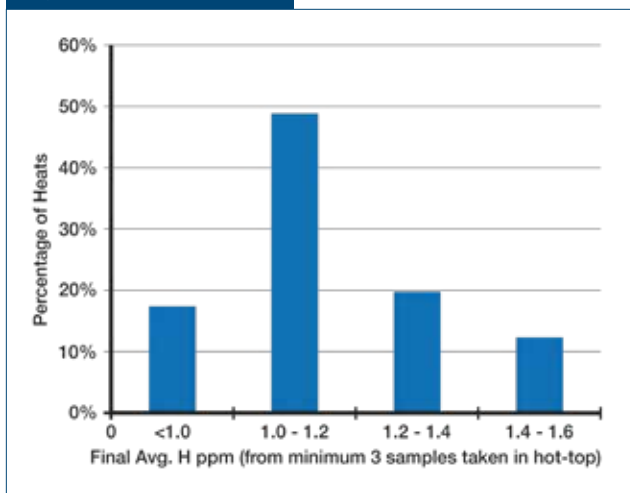
- Specific ladle scheduling rules to ensure previous liquid steel exposure to inner nozzle, slide-gate and collector nozzle.
- Vacuum treatment at <1 mbar pressure with combined EMS and Ar gas stirring.
- Strict limitations on alloying and slag additions after vacuum treatment.
- Argon shrouding of the lower ladle stream.
- Ladle-to-ladle shrouding of the upper ladle stream(s).
- Pre-heating of bottom pour refractory to 500°C.
- Proper pre-heating of mold.
- Flux addition by pouring directly into hot mold for residual moisture removal.

The ultralow-hydrogen practices have resulted in an average of 35% reduction in hydrogen pickup during bottom pouring. Fig. 19 shows the hydrogen pickup for standard processing (including testing just prior to bottom pouring for comparison) and the ultralow-hydrogen practice. Fig. 20 shows the distribution of final hydrogen analyses from sandwich-poured ingots at EQS, as reported previously.⁴

References

1. J.R. Paules, W.P. Edwards and B.E. Gabrielson, "VOD Processing of Forged Precipitation Hardening Stainless Steels," *IFM*, Tokyo, 2014.
2. B.E. Gabrielson and R.E. Rumcik, "Start Up of the ASEA-SKF Secondary Steelmaking Unit at EUS," *AISE Annual Conference*, 1986.
3. B.M. Connolly and B.E. Gabrielson, "Process Control and Quality Assurance During the Production of High-Quality Bottom-Poured Ingots at Ellwood Quality Steels," *1st ICRF*, Aachen, Germany, 2012.
4. B.E. Gabrielson, R.O. Olivares, B.M. Connolly, D. Schwartz and W. Zaben, "Development, Implementation and Results of Large Bottom-poured Ingots at Ellwood Quality Steels," *20th International Forgemasters Meeting*, Graz, Austria, 2017.
5. R.J. Fruehan, "A Review of Hydrogen Flaking and Its Prevention," *ISS Transactions*, August 1997.
6. Correspondence between J.P. Hirth (Washington State University) and R.E. Rumcik (Ellwood Quality Steels), 22 August 1996.
7. J.P. Hirth, "Effects of Hydrogen on the Properties of Iron and Steel," *Metallurgical Transactions A*, Vol. 11A, June 1980.
8. K. Thelning, *Steel and Its Heat Treatment*, 2nd Edition, Butterworth, London, U.K., 1984.
9. B.E. Gabrielson, "Vacuum Treatment of Liquid Steel at Ellwood Quality Steels — A Function Description," EQS internal publication, November 2013.
10. B.E. Gabrielson and S.F. Lubinski, "The Control of Hydrogen During Production of Forging Ingots at Ellwood Uddeholm Steel Company," *9th International Vacuum Metallurgy Conference*, San Diego, Calif., USA, 1988.
11. T. Hsiao, T. Lehner, B. Kjellberg, "Fluid Flow in Ladles — Experimental Results," *Scandinavian Journal of Metallurgy*, Vol. 9, No. 3, 1980.
12. H. Ohmori et al., "Making of 200-Ton-Max Forging Ingot by Bottom Pouring With LD-RH Process," Mizushima Works, Kawasaki Corp., 1981. ◆

Figure 20



Histogram of final hydrogen content in sandwich-poured ingots at EQS.